Ore Geology Reviews 146 (2022) 104931

Contents lists available at ScienceDirect

Ore Geology Reviews

journal homepage: www.elsevier.com/locate/oregeorev

Granitic magma evolution to magmatic-hydrothermal processes vital to the generation of HREEs ion-adsorption deposits: Constraints from zircon texture, U-Pb geochronology, and geochemistry

Xu Zhao [a,b], Ning-Bo Li [a,b,*], Jan Marten Huizenga [c,d,e], Qi-Bing Zhang [a,b,f], Yu-Yuan Yang [a,b], Shuang Yan [a,b], Wu-bin Yang [a,b], He-Cai Niu [a,b]

[a] CAS Key Laboratory of Mineralogy and Metallogeny/Guangdong Provincial Key Laboratory of Mineral Physics and Materials, Guangzhou Institute of Geochemistry, Chinese Academy of Sciences, Guangzhou 510640, China
[b] CAS Center for Excellence in Deep Earth Science, Guangzhou 510640, China
[c] Faculty of Environmental Sciences and Natural Resource Management, Norwegian University of Life Sciences, P.O. Box 5003, NO-1432 Ås, Norway
[d] Economic Geology Research Institute (EGRU), College of Science and Engineering, James Cook University, Townsville, Queensland 4811, Australia
[e] Department of Geology, University of Johannesburg, P.O. Box 524, Auckland Park 2006, South Africa
[f] No. 6 Institute of Geology and Mineral Resources Exploration of Shandong Province, Shandong 264200, China

ARTICLE INFO

Keywords:
Heavy rare earth elements
HREE ion-adsorption deposits
Zircon
Granites

ABSTRACT

The key point for further prospecting of heavy rare earth elements (HREE) ion-adsorption deposit is to figure out the granites that could generate HREE ion-adsorption mineralization in weathering processes. In this study, we present a detailed study of zircons from granites associated with Zudong, Dabu, and Xinfeng HREE ion-adsorption deposits in South China. The zircons were studied with regards to their texture, crystallinity, U-Pb dating, and geochemistry. The zircons from these granites all can be subdivided into two types. The type-1 zircons show oscillatory zonation and have Th/U and Zr/Hf mass ratios of 0.4–1.0 and 30–50, respectively. These textural and geochemical features indicate crystallization in a fractionated magma. The type-2 zircons are unzoned, occasionally porous, and have a low crystallinity. They occasionally rim type-1 zircons. The type-2 zircons show significantly higher F, P, Hf, Th, U, and REE contents, but display lower ZrO_2 and SiO_2 contents and lower Th/U, Zr/Hf, La/Yb ratios than those of the type-1 zircons. These geochemical features are consistent with zircon formation in a volatile-HREE-rich magmatic-hydrothermal transition stage. Under these conditions, the HREEs were also hosted in volatile-rich REE mineral phases including synchysite-(Y), aeschynite-(Y), calcybeborosilite-(Y), and atelisite-(Y), which have been observed in these HREE deposits. These volatile-rich REE-mineral phases can easily be dissolved during weathering and release $HREE^{3+}$ to generate ion-adsorption HREE deposits. Therefore, we conclude that the granitic magma progression to a volatile-HREE-rich magmatic-hydrothermal system is vital for the generation of HREE ion-adsorption deposits. The long-term Mesozoic extension of the South China favors the generation of highly fractionated granites and is thus important for the generation of HREE ion-adsorption deposits. Furthermore, the zircons generated in a volatile-rich environment could be used to determine the HREE ion-adsorption mineralization potential of granites.

1. Introduction

Rare earth elements (REEs) are defined as critical metals owing to their irreplaceable application in renewable-energy and high-technology products (Chakhmouradian and Wall, 2012; Fan et al., 2020). Heavy REEs (HREE: Gd-Lu + Y) are considered to be more critical than the light REEs (LREE: La-Eu) due to their comparatively lower crustal abundance (Rudnick and Gao, 2003; Sanematsu and Watanabe, 2016). Globally, most HREEs are derived from ion-adsorption deposits in South China (Li et al., 2017). The ion-adsorption REE deposits, especially the HREE-dominated deposits, typically occur in the weathering profile of granitic rocks (e.g. Bao and Zhao, 2008; Sanematsu and

* Corresponding author at: Key Laboratory of Mineralogy and Metallogeny, Guangzhou Institute of Geochemistry, Chinese Academy of Sciences, 511 Kehua Street, Tianhe District, Guangzhou 510640, China.
E-mail address: liningbo@gig.ac.cn (N.-B. Li).

https://doi.org/10.1016/j.oregeorev.2022.104931
Received 23 September 2021; Received in revised form 21 March 2022; Accepted 9 May 2022
Available online 13 May 2022

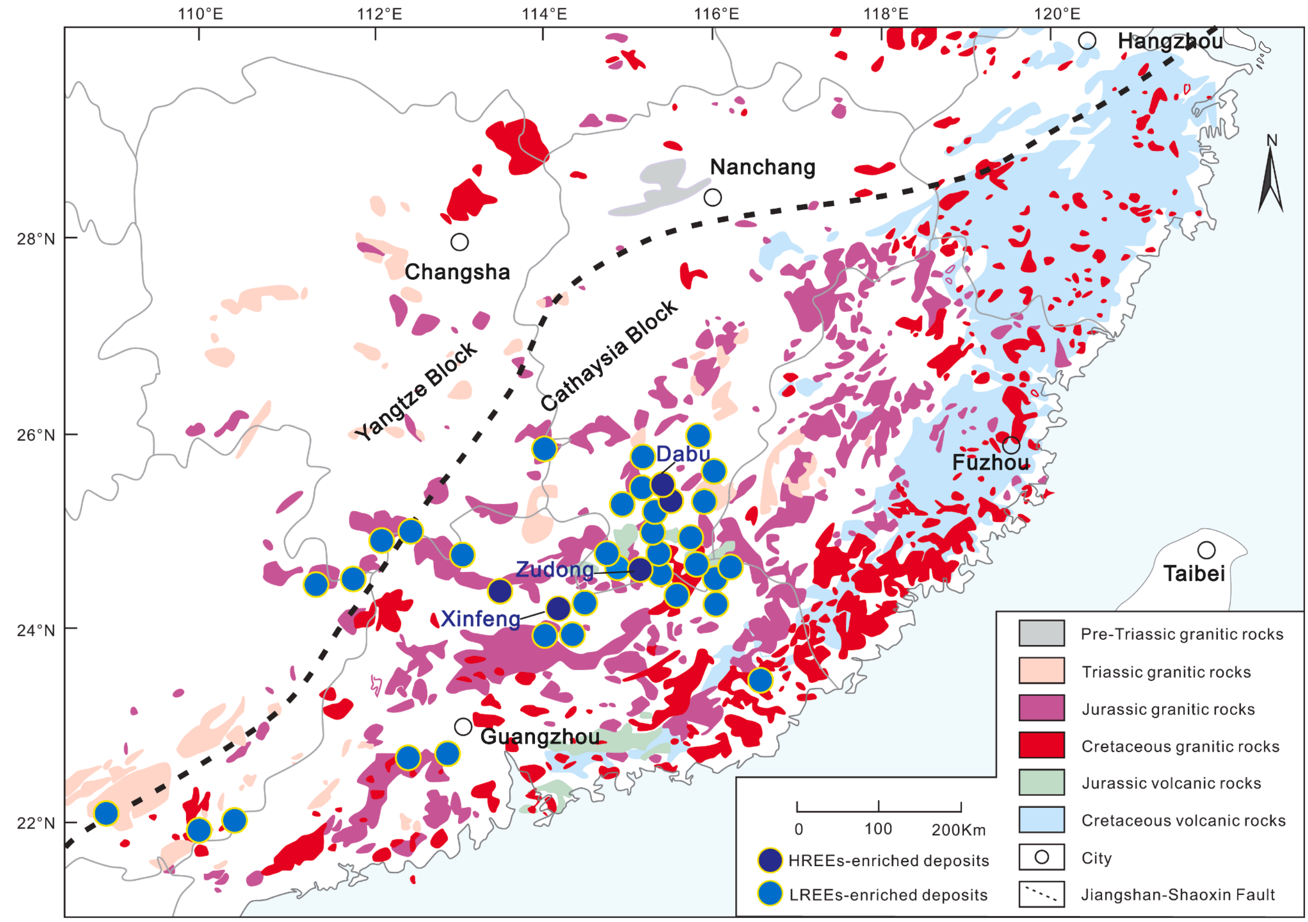

Fig. 1. Geological map of South China showing the distributions of the middle to large scale ion-adsorption deposits. The locations of the deposits are from Li et al., 2017 and references therein.

Watanabe, 2016; Li et al., 2019). Previous studies have indicated that the chemical weathering in a warm and humid climate like that in South China, is critical for ion-adsorption REE mineralization (Tang and Johannesson, 2010; Sanematsu et al., 2013; Fu et al., 2019; Li et al., 2019). However, only less than 10% of the defined ion-adsorption deposits are dominated by HREEs (Fig. 1), which is characterized by a high HREE/LREE ratio and locally occur in the weathering profile of the granitic complexes (Huang et al., 1989; Li et al., 2017). It is suggested that although the supergene process is vital to the generation of the HREE ion-adsorption deposits, the weathering typically causes LREE enrichment relative to HREE (Yusoff et al., 2013; Xu et al., 2017). This implies that the formation of HREE-dominated ion-adsorption deposits should be also controlled by the HREE contents and REE pattern of the parent granites. Therefore, in order to improve prospecting of the HREE ion-adsorption deposits, it is essential to determine (1) which granitic rocks have the potential to generate the HREE deposits during weathering, and (2) why some granitic rocks are related to the HREE mineralization whereas others are related to LREE mineralization or are not mineralized despite in the similar weathering conditions.

Zircon is the main HREE-hosted accessory mineral in the granites and the zircon structure and composition are not affected by weathering process, i.e. the zircon geochemistry can be used to decipher the magmatic and hydrothermal processes (Middelburg et al., 1988; Hoskin, 2005; Pettke et al., 2005; Zeng et al., 2017; Yang et al., 2014). Therefore, zircons may provide relevant information for the evaluation of the HREE mineralization potential for granitic rocks. In this study, we present the results of a detailed zircon study (i.e., texture, crystallinity, U-Pb geochronology, and geochemistry) from three giant, well-known HREE-dominated ion-adsorption deposits in South China, i.e. the Zudong, Dabu, and Xinfeng deposits (Figs. 1, 2). The aim of this study is to identify the factors that promote HREE enrichment in these granites and to provide guidance to the prospecting of HREE-dominated ion-adsorption deposits.

2. Geological background and petrography

South China is subdivided into the Yangtze block in the northwest and the Cathaysia Block in the southeast, separated from each other by the Jiangshan-Shaoxin Fault (Fig. 1; Li et al., 2008; Tao et al., 2018). The tectono-magmatic events in the South China occurred during Paleozoic to Mesozoic. The Paleozoic orogeny in South China associated with the continental collision between the Cathaysia Block and Yangtze Block probably started as early as in the Middle Ordovician with peak deformation at 460–440 Ma (Charvet et al., 2010). Subsequent post-orogenic extension (440–400 Ma) was accompanied by widespread formation of granitic rocks (Faure et al., 2009; Li et al., 2017). During the Late Permian to Triassic, numerous syn-orogenic granites were generated due to the collision between the Indochina and South China Blocks, and the collision between the North China and the South China Block (Zheng et al., 2009; Fan et al., 2010). Subsequently, South China was characterized by the flat subduction of the Paleo-Pacific Ocean during the Jurassic (Li and Li, 2007; Mao et al., 2013) and subsequent Late Jurassic to Cretaceous extension caused by the slab foundering and an abrupt increase of the dip angle of the subducting slab (Zhou et al., 2006; Chen et al., 2016).

The Cathaysia Block in South China is the main region that contains numerous ion-adsorption REE deposits. Most of the ion-adsorption REE deposits are hosted in the weathered profile of the granitic rocks

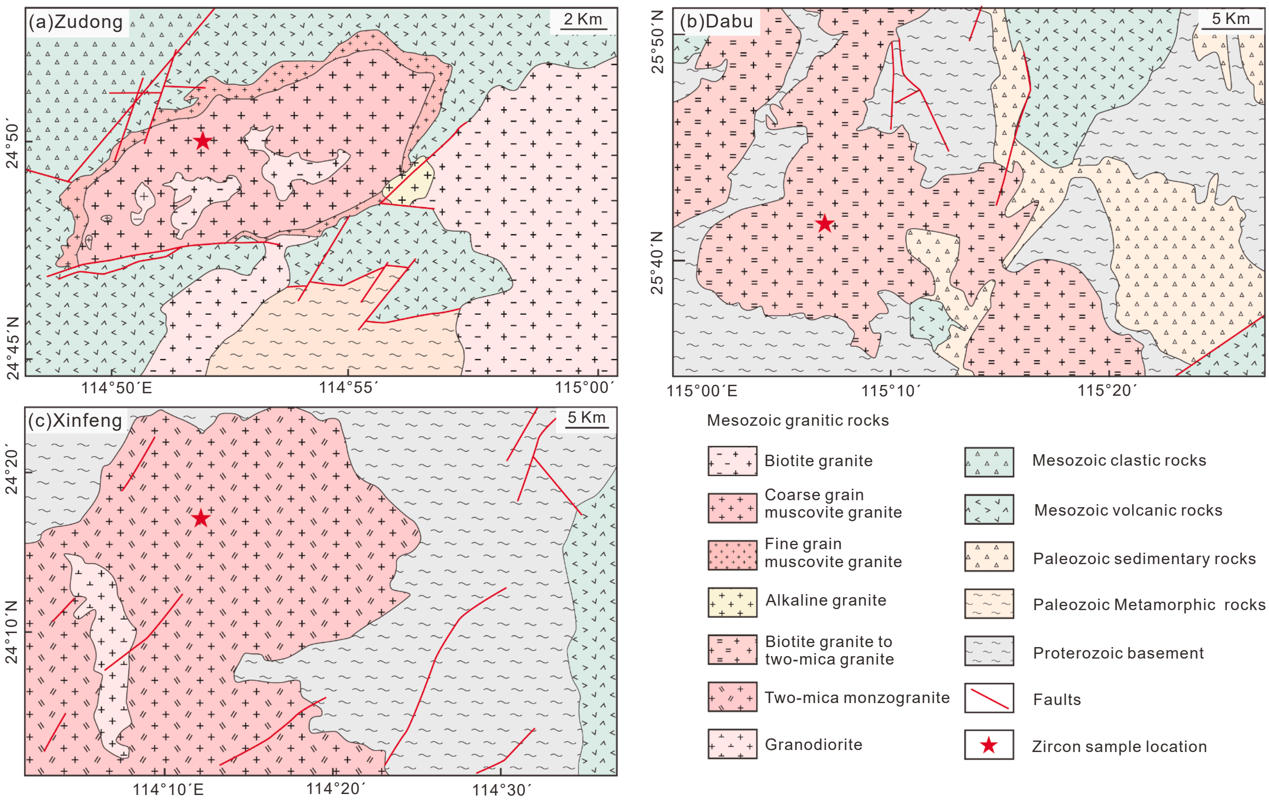

Fig. 2. Simplified geological map showing the distribution of granites in (a) Zudong, (b) Dabu, and (c) Xinfeng area.

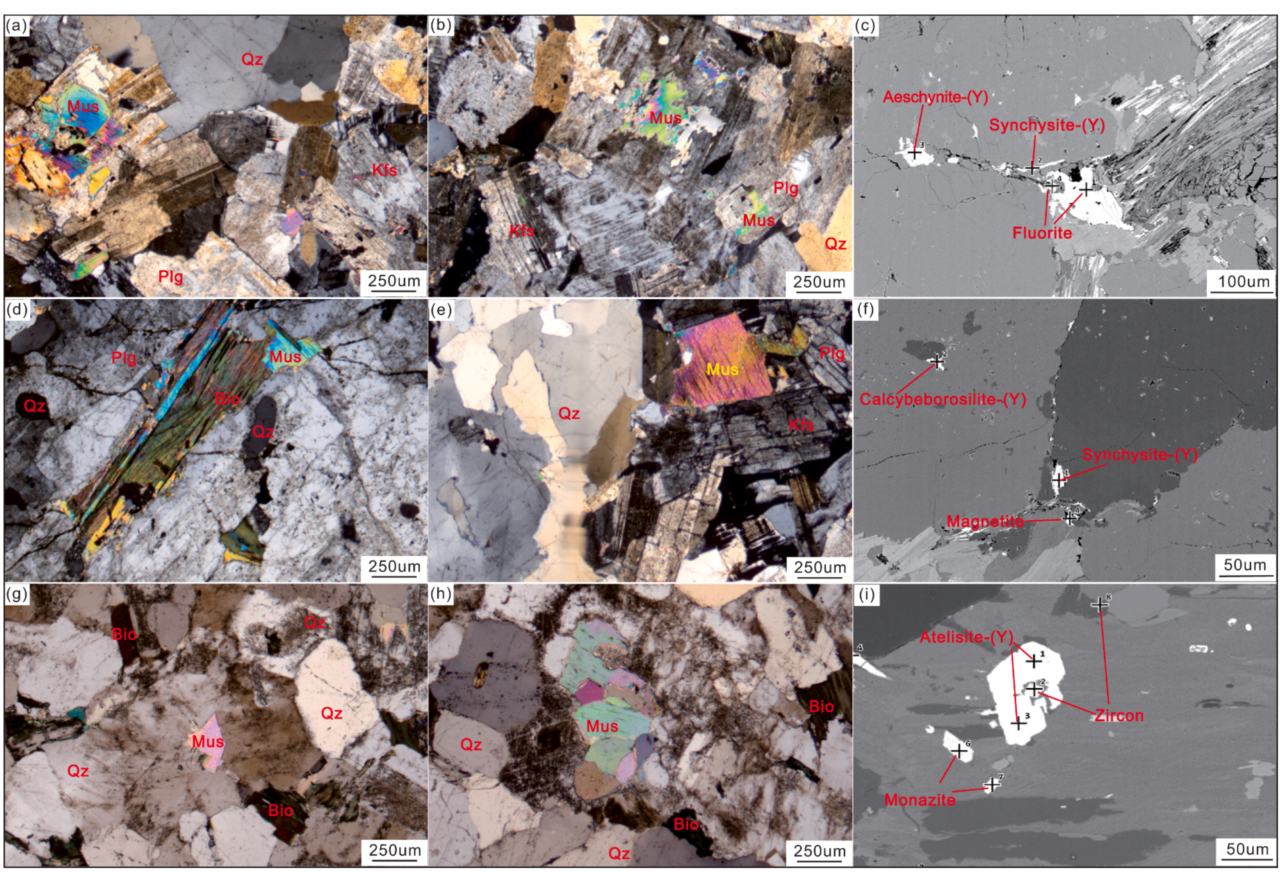

Fig. 3. Photomicrographs of (a-c) Zudong muscovite granite, (d-f) Dabu two-mica granite and (g-i) Xinfeng two-mica monzogranite.

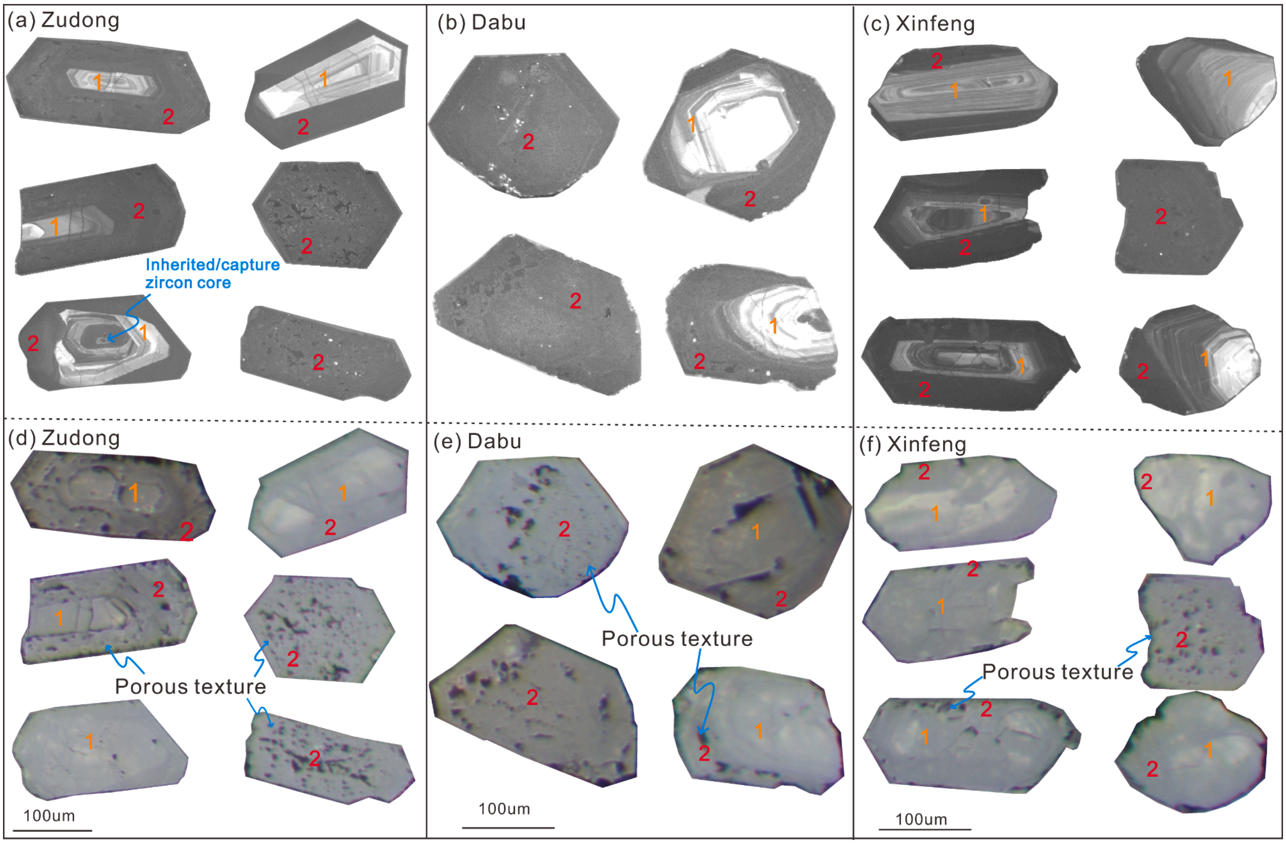

Fig. 4. Photomicrographs showing the two types of zircons (1 represent type-1 zircon and 2 represent type-2 zircon). The zircons in the first line from (a-c) are cathodoluminescence images and in the second line are corresponding images under reflected light.

whereas a few deposits are also related to the rhyolitic tuff (Wang and Ruan, 1989), lamprophyres (Bao and Zhao, 2008), basalts (Zhang et al., 2016), and metamorphic rocks (Huo, 1992). The granites associated with ion-adsorption deposits are either Silurian or Jurassic-Cretaceous in age (Zhang et al., 2015; Li et al., 2017). The granites are generally calc-alkaline with ΣREE contents ranging from 110 to 590 ppm (Sanematsu and Watanabe, 2016). It is noticeable that only a small part (<10%) of the ion-adsorption deposits are HREE-enriched (Fig. 1). Those granites related to HREE ion-adsorption deposits are characterized by high SiO_2 contents and high differentiation index (Huang et al., 1989; Li et al., 2017).

The giant Zudong HREE deposit comprises more than 17,622 t of REE oxide (Li et al., 2017). Late Jurassic granitic rocks distributed in the Zudong area intruded into Triassic volcanic rocks (Fig. 2a) and crop out in an area of 4 by 9 km along NNE-SSW trending faults (Fig. 2a). The rocks include medium- to coarse-grained biotite granite and fine- to coarse-grained muscovite granite. The muscovite granites are the parent rocks for the HREE-rich ion adsorption mineralization whereas the weathering profile of the biotite granite are generally richer in LREEs (Huang et al., 1989). The muscovite granites consist of quartz (35%-45%), K-feldspar (20–25%), albite (20–35%), and muscovite (5–10%). Accessory minerals include zircon, apatite, fluorite, topaz, synchysite-(Y), aeschynite-(Y), monazite, gadolinite, xenotime, and fergusonite (Fig. 3a-c; Huang et al., 1989; Li et al., 2017). Synchysite-(Y) has been considered to be an important mineral in the Zudong granite, which contributed to the HREE enrichment during weathering (Huang et al., 1989; Bao and Zhao, 2008).

The Dabu HREE-enriched ion-adsorption deposit is situated in the Dabu pluton, which comprises dominantly (>99.5%) Late Jurassic biotite granite and two-mica granite within an outcrop area of more than 400 km^2 (Fig. 2b; Wang, 2015; Wu et al., 2017a). The HREE mineralization locally occurs in the weathering profile of the two-mica granite, which consists of quartz (30–50%), K-feldspar (20–30%), plagioclase (10–15%), biotite (5–10%), muscovite (5–10%), with accessory minerals of zircon, apatite, fluorite, xenotime, magnetite, fergusonite, thorite, calcybeborosilite-(Y), and synchysite-(Y) (Fig. 3d-f, Wu et al., 2017a).

The Xinfeng ion-adsorption deposit is a medium to large scale HREE-enriched deposit. The Xinfeng granite includes two-mica monzogranite and granodiorite (Fig. 2c). The two-mica monzogranite hosts the HREE ion-adsorption mineralization and comprises quartz (30–35%), K-feldspar (30–35%), plagioclase (25–30%), biotite (5–10%), muscovite (5–10%), and accessory minerals of zircon, apatite, xenotime, monazite, magnetite, fluorite, and atelisite-(Y) (Fig. 3g-i).

3. Analytical methods

Zircon grains for U-Pb dating and elemental analyses were separated by conventional magnetic and density techniques at Guangzhou Tuoyan Testing Technology Co. Ltd. The zircons were handpicked and embedded in epoxy resin and polished to expose the core. The zircons were picked from samples ZD-1 (Zudong granite), 20DB-1-1 and 20DB-2-1 (Dabu granite), and XF-3 (Xinfeng granite). Zircons without visible fractures were selected for cathodoluminescence (CL) imaging using the FEI NOVA NanoSEM 450 scanning electron microscope equipped with a Gatan Mono CL4 cathodoluminescence system at the Guangzhou Tuoyan Testing Technology Co., Ltd.

Laser Raman analyses were conducted at the Chinese Academy of Sciences (CAS), Key Laboratory of Mineralogy and Metallogeny, Guangzhou Institute of Geochemistry (GIG), Guangzhou (China), using a HORIBA XploRA Plus Laser Raman micro-spectroscope. An Ar ion laser operating at 10 mW was used to produce the excitation wavelength of 532 nm. The beam was coupled with a grating of 1200 gr/mm. The system was calibrated daily using silicon with a Raman peak at 520.7

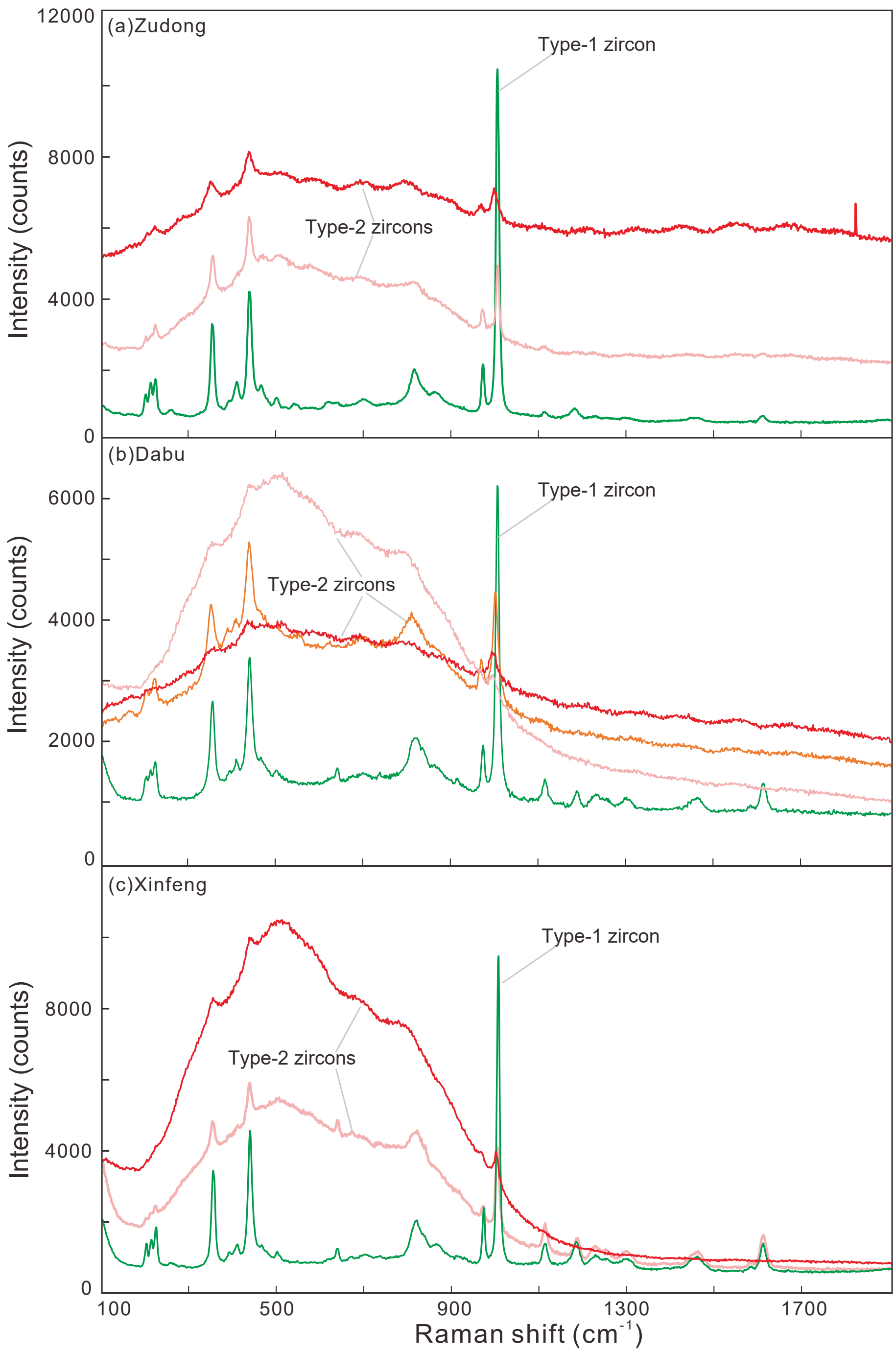

Fig. 5. Raman spectroscopy for type-1 and type-2 zircons from the Zudong, Dabu, and Xinfeng granites that are associated with HREE ion-adsorption mineralization.

cm^{-1} yielding a wavenumber accuracy of about ± 1 cm^{-1}. All measurements were done using a 100 μm entrance slit and 100 μm confocal pin hole.

Zircon major element analyses were conducted at the Key Laboratory of Mineralogy and Metallogeny at GIG using a JEOL JXA 8230 electron microprobe analyses (EMPA). A focused beam with an accelerating voltage of 25 kV and a current of 20 nA was used for the analyses. Standards for different elements including zircon for Zr and Si, apatite for P, rutile for Ti, monazite for Y, Th and U, and magnetite for Fe. The detection limits are 0.01–0.02 wt% for these elements.

Zircon U-Pb dating and trace element point analyses were performed at the CAS Key Laboratory of Mineralogy and Metallogeny, in GIG using a 193 nm GeoLasPro and Agilent 7900 ICP-MS with a laser spot size of 29 μm. The frequency of the laser was set at 8 Hz. Argon was used as the make-up gas mixed helium (carrier gas) via a T-connector before entering the ICP. The samples 91500 zircon and NIST610 glass were used as an external standard for U-Pb dating and trace element calibration, respectively. Zircon trace elemental mappings were also conducted using a 193 nm GeoLasPro and Agilent 7900 ICP-MS at GIG. The spot size was 9 μm and laser frequency was set at 8 Hz. Line analyses of NIST610 done every ~8 min before and after the zircon mapping were used as an external standard. The data processing and mapping were performed using Iolite 4.0.

Granite whole-rock major element analysis was done by using a Primus II (Rigaku, Japan) X-ray fluorescence (XRF) at the Wuhan Sample Solution Analytical Technology Co., Ltd (WSSAT). The error for

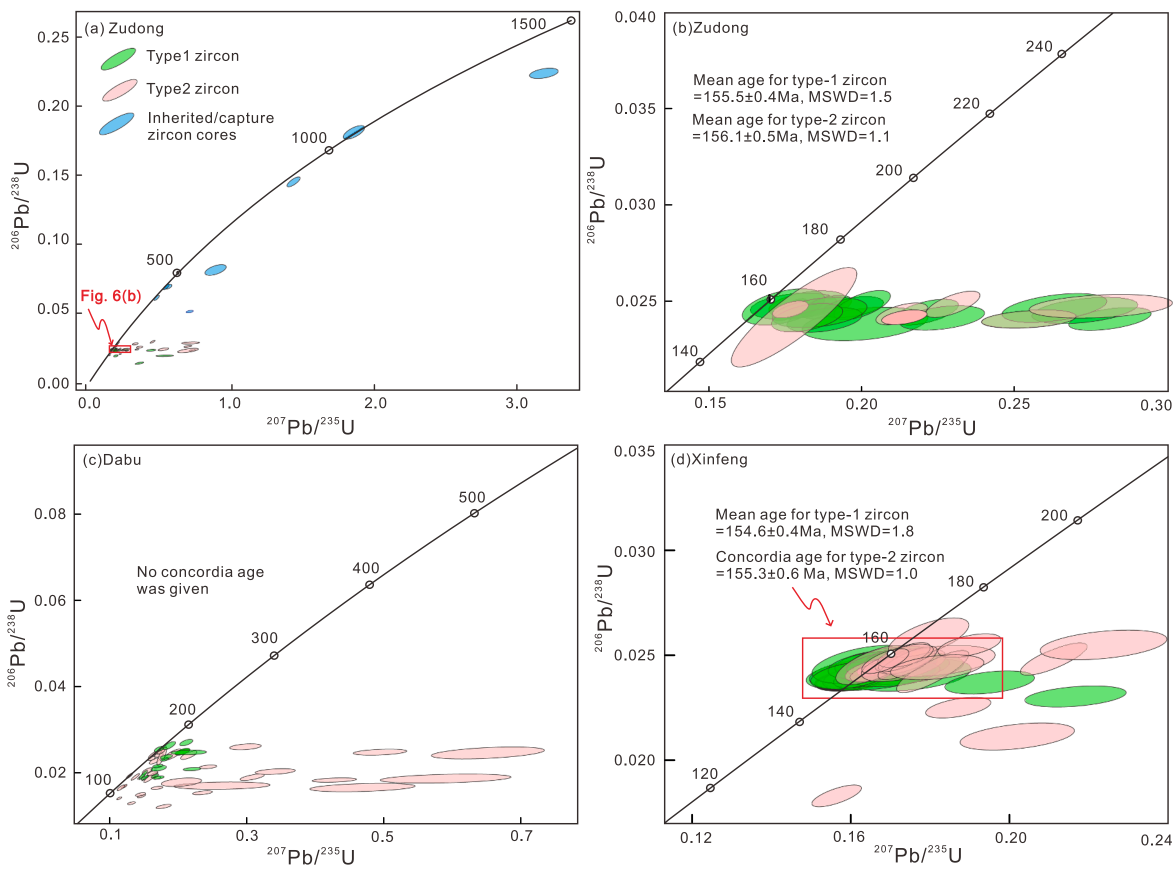

Fig. 6. Zircon U-Pb concordia plots for (a-b) Zudong, (c) Dabu, and (d) Xinfeng granites.

the major element analysis is <5%. The trace elements were analyzed using an Agilent 7700e ICP-MS at WSSAT. The sample powder was weighed and placed in a Teflon bomb after drying of 12 h in an oven at 105 °C. The sample powders were digested in a HF-HNO_3 solution in Teflon bombs, which were subsequently put in a stainless-steel pressure jacket and heated to 190 °C in an oven for >24 h. The final solution was transferred to a polyethylene bottle and diluted to 100 g using 2% HNO_3. The error for the trace element analysis is <2%.

4. Results

4.1. Zircon texture and crystallinity

Zircons from the Zudong, Dabu, and Xinfeng granites are 100–250 μm in length with length-width ratios between 1 and 3 (Fig. 4). Zircons from the granites in these different deposits have similarities as they all can be subdivided into two types (type-1 and type-2) according to their mineralogical characteristics and CL appearance (Fig. 4). Type-1 zircons are euhedral, exhibit oscillatory zoning in CL imaging, and a well-defined Raman peak at ~1008 cm^{-1}, indicating a high crystallinity (Fig. 5). Type-2 zircons are dark and do not show oscillatory zoning. They occasionally rim type-1 zircons and exhibit a porous texture (Fig. 4). The Raman peak at ~1008 cm^{-1} is either weak or absent, indicating a low crystallinity (Fig. 5). In addition, the type-1 zircons from the Zudong granite occasionally show a more complex texture as they contain inherited/captured zircon cores.

4.2. Zircon U-Pb geochronology

The data for zircon U-Pb dating is given in supplementary Table S1 and illustrated in Fig. 6. The type-1 zircon in Zudong granites have variable Th and U contents of 63–2706 and 243–10,090 ppm, respectively, and Th/U mass ratios of 0.15–0.91 (mostly > 0.40). The type-2 zircons in Zudong granites show higher Th (852–45,412 ppm) and U contents (5396–45,486 ppm), and lower Th/U mass ratios (0.07–0.56, mostly < 0.40). Both zircon types (but in particular type-2 zircons) experienced common Pb loss and deviate from the U/Pb concordia line. Type-1 and type-2 zircons that did experience minimal loss of common Pb still yield ages of 155.5 ± 0.4 Ma (MSWD = 1.5) and 156.1 ± 0.5 (MSWD = 1.1), respectively, indicating that the type-1 and type-2 zircons have the same Late Jurassic age (Fig. 6a-b). In addition, the internal zircon cores within the type-1 zircons from the Zudong granites show older ages of 322–1293 Ma (Fig. 6a), indicating that they were inherited or captured.

In the Dabu granites, the type-2 zircons also show higher Th, U and lower Th/U ratios than those of the type-1 zircons. However, the most zircons show significant loss on common Pb and could not give a concordant age, but the type 2 zircons generally have the same age distribution with the type 1 zircons as shown in the U-Pb plots (Fig. 6c). With regard to the zircons from the Xinfeng granites, the zircons also show same changes of Th, U contents and Th/U ratios from type-1 zircons to type-2 zircons as those in the Zudong and Dabu granite. Most type-1 and type-2 zircons experienced a minimal loss of common Pb yielding a U-Pb Late Jurassic ages of 154.6 ± 0.4 Ma (MSWD = 1.8) and 155.3 ± 0.6 Ma (MSWD = 1.0), respectively (Fig. 6d).

4.3. Zircon major and trace element geochemistry

Zircon major and trace element compositions from the Zudong, Dabu and Xinfeng granites are given in Tables S2 and S3 and illustrated in Figs. 7–10. The type-1 zircons from the Zudong granite show a consistent major element geochemistry with ZrO_2 contents of 62.01–63.93 wt %, HfO_2 contents of 1.16–1.75 wt%, SiO_2 contents of 32.43–33.14 wt%, and Y_2O_3 contents of 0.12–0.51 wt%. The P_2O_5 and F contents are

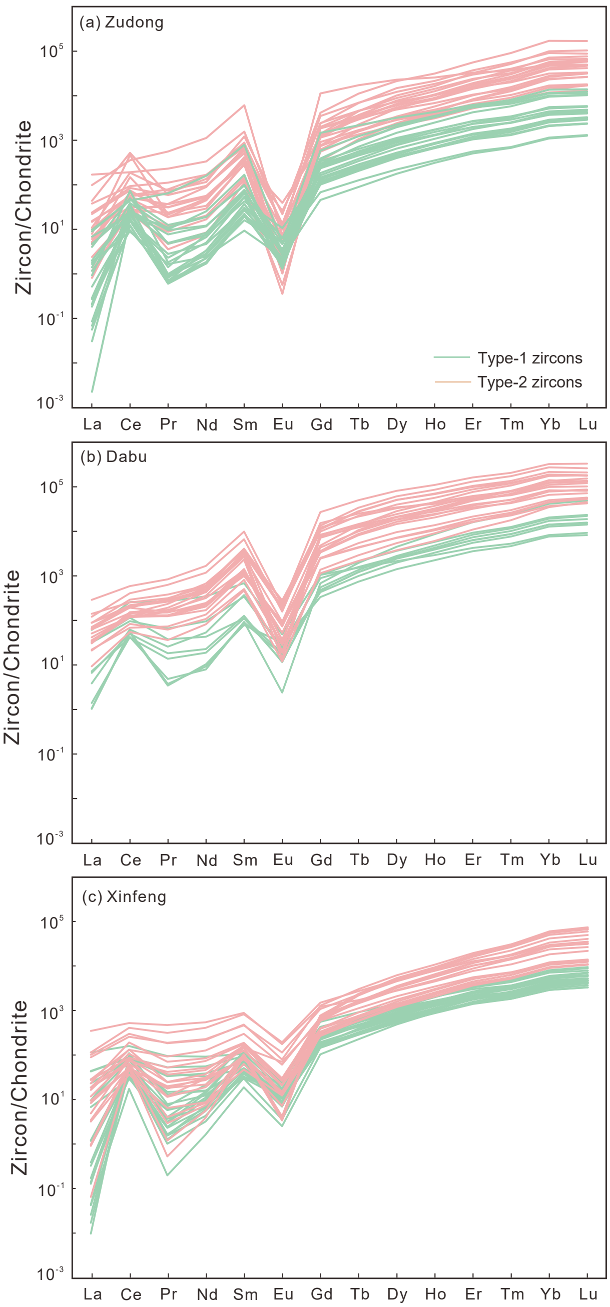

Fig. 7. Normalized REE patterns for type-1 (green) and type-2 (red) zircons from Zudong, Dabu, and Xinfeng granites. Chondrite values are from Sun and McDonough (1989).

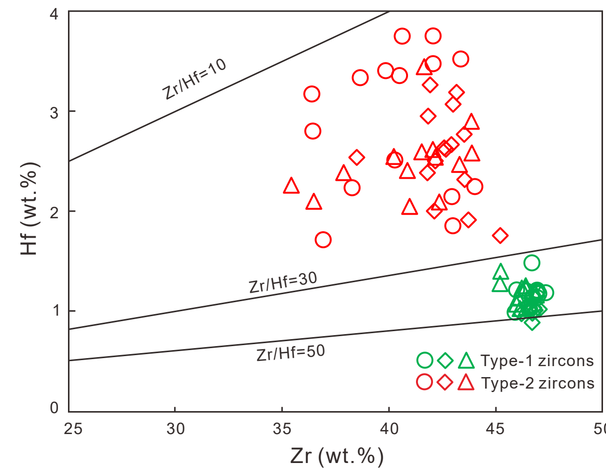

Fig. 8. Zr vs. Hf for type-1 (green) and type-2 (red) zircons from the Zudong (circles), Xinfeng (triangles), and Dabu (diamonds) granites.

generally below the detection limit. The total weight of the EMPA ranges between 96.34 and 98.90 wt%.

The type 2 zircons from the Zudong granite show a more variable and lower ZrO_2 (49.17–59.47 wt%) and SiO_2 contents (27.04–32.24 wt%), and higher HfO_2 (2.02–4.42 wt%), Y_2O_3 (0.58–3.68 wt%), and P_2O_5 contents (0.11–2.90 wt%). The F contents for the type-2 zircons from the Zudong granites is up to 0.27 wt% and the total weight of the EMPA ranges between 87.13 and 96.58 wt% (mostly higher than 92.00 wt%). The type-2 zircons show higher trace element contents than the type-1 zircons, especially for the Th, U, and REE contents. In addition, the type-2 zircons show lower Th/U, and Zr/Hf ratios (Figs. 7–9) and have a more pronounced negative Eu anomaly than the type-1 zircons (Fig. 7).

The inherited/captured zircons core within the type-1 zircons from Zudong granite have variable trace element compositions, but their REE, Nb, Ta, Th, and U contents are generally lower than those of Type-2 zircons and are higher than those of the type-1 zircons (Table s3, Fig. 10). The geochemical compositions of these inherited/captured zircon cores are inherited from their source area and do not reflect the magmatic evolution process and, therefore, are not compared with the type-1 and type-2 zircons in Figs. 6–9.

With regard to the zircons from the Dabu and Xinfeng granites. The geochemical characteristics for the type-1 and type-2 zircons are similar to those of the type-1 and type-2 zircons from the Zudong granite. Generally, the type-2 zircons show lower ZrO_2, SiO_2, and total weight of the EMPA, but display higher HfO_2, Y_2O_3, P_2O_5, and F contents than the type-1 zircons. This chemical variation in the type-2 zircons probably resulted from a xenotime-type substitution [(Y, REE)$^{3+}$ + P^{5+} → Zr^{4+} + Si^{4+}] (Kelly et al., 2020; Dou et al., 2021). The type-2 zircons also show higher Th, U, and REE contents, lower Th/U and Zr/Hf ratios, and a more pronounced negative Eu anomaly than the type-1 zircons (Figs. 7–9). Furthermore, it is noteworthy that the REEs in the type-2 zircons from the three granites do not show the predicted charge-and-radius-controlled (CHARAC) behavior (Fig. 9g–i) whereas the type-1 zircons in the Zudong and Xinfeng granites do show CHARAC behavior.

4.4. Whole rock major and trace element geochemistry

Whole-rock composition for the Mesozoic granites associated with HREE mineralization in the Zudong, Dabu and Xinfeng area are presented in Table S4. The three granites are characterized by high SiO_2 (73.13–76.70 wt%) and K_2O (4.26–5.76 wt%) contents, and low Na_2O/K_2O mass ratios (0.46–0.95). All three granites show insignificant LREE/HREE fractionation, i.e. $(La/Yb)_N$ ratios of 0.25–5.92 (only one value > 2), and a negative Eu anomaly (Eu/Eu* ratios of 0.01–0.21) (Fig. 11a). The three granites show relatively low Zr/Hf (13.1–27.6), Nb/Ta (4.37–9.21), and K/Rb mass ratios (44.7–102.5) (Fig. 11b).

5. Discussion

5.1. Zircon genesis

The zircons from the three granites show similar texture with occurrence of both the type-1 and type-2 zircons. Although there are extra zircon cores within the type-1 zircons from the Zudong granite, they are inherited from magmatic source or captured from country rocks with older ages (Fig. 6a), rather than crystallize in the magmatic processes. In contrast, the type-1 and type-2 zircons show similarly younger Late Jurassic U-Pb ages and could either be magmatic or hydrothermal in origin (Hoskin and Schaltegger, 2003).

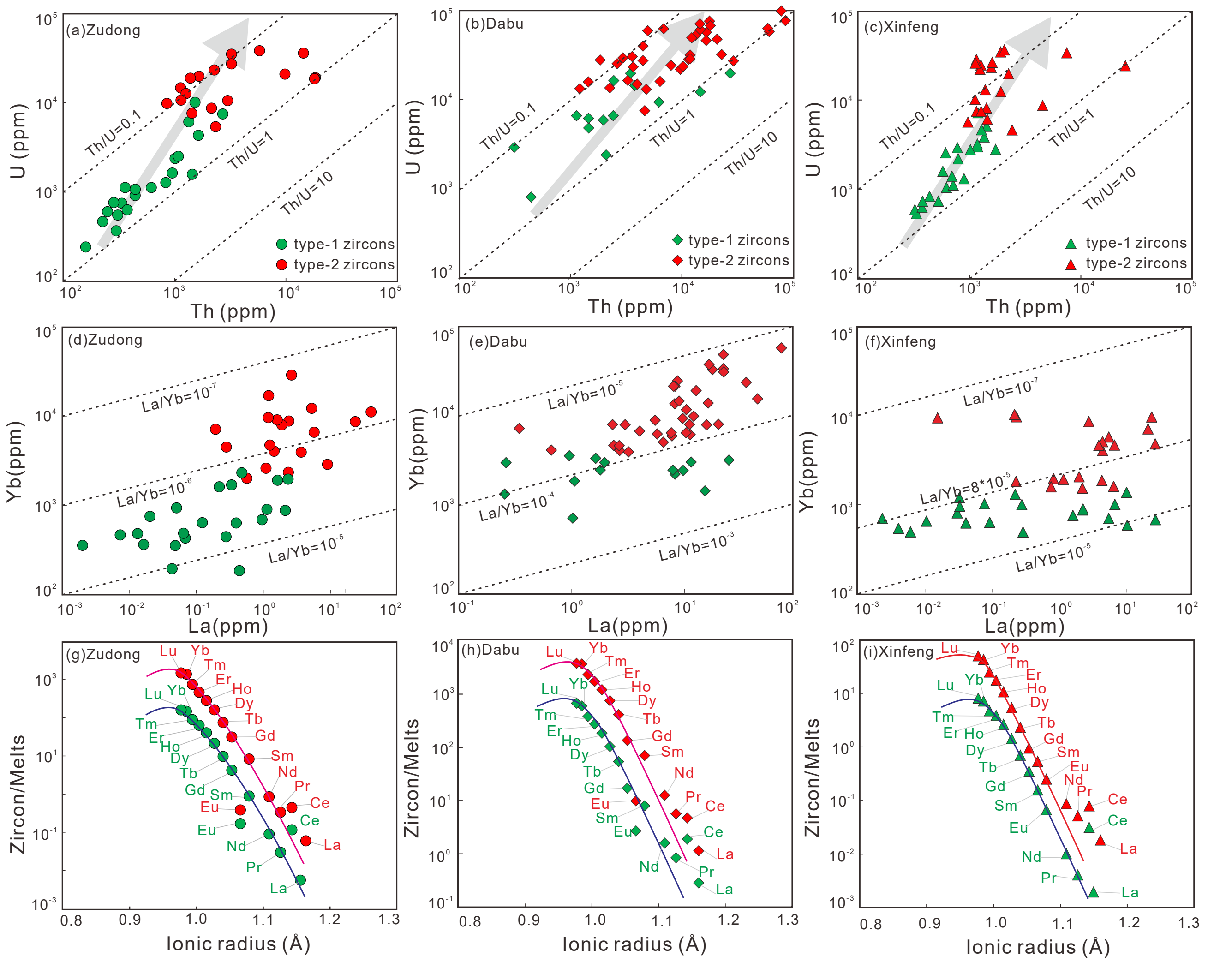

Fig. 9. Diagrams showing (a-c) U vs. Th, (d-f) Yb vs. La, and (g-i) partition coefficient of REEs vs. ionic radius for type-1 (green) and type-2 (red) zircons from the Zudong, Dabu, and Xinfeng granites.

Magmatic zircons usually show oscillatory zonation due to the low diffusion rate of trace elements in the zircon at a relatively low temperature and high viscosity conditions for the acid magma (Zeng et al., 2017). The type-1 zircons from the Zudong, Dabu and Xinfeng HREE deposits all show oscillatory zonation and Th/U ratios generally > 0.4 (Table S1; Fig. 4, 9a-c), indicating a magmatic origin (Hoskin and Schaltegger, 2003). The well-defined Raman peak at ~1008 cm^{-1} (Fig. 5) is indicative of highly crystalline magmatic zircon (e.g., Yang et al., 2014; Zeng et al., 2017). Furthermore, the type-1 zircons are characterized by Th/U mass ratios < 1 and Zr/Hf mass ratios < 50, which is consistent with its formation in a relatively fractionated magma (Wang et al., 2010; Černý et al., 2012; Yan et al., 2020).

Type-2 zircons occur as individual grains or as rims around type-1 zircons, indicating that type-2 zircons were formed after the type-1 zircons (Fig. 4). Generally, the type-2 zircons are irregular and low-luminescent without visible zoning. They show a distinct porous texture and a weak or invisible Raman peak at ~1008 cm^{-1} (Figs. 4–5) which is characteristic for a low-crystallinity metamict zircon (e.g. Erdmann et al., 2013; Hoskin, 2005; Pettke et al., 2005; Yang et al., 2014; Zeng et al., 2017). We propose that the generation of the type-2 metamict zircons is associated with a fluid exsolved from the magma during volatile-rich magmatic-hydrothermal stage. This hypothesis is supported by the following: (1) No evidence for metamorphism and deformation was found in the zircons-hosted granites, i.e. metamorphism cannot account for the origin of the metamict zircons. (2) The type-2 zircons show higher Th and U contents (up to tens of thousands ppm), which is consistent with hydrothermal system rather than a metamorphic origin (e.g. Qu et al., 2019). It is suggested that very high U and Th concentrations in zircons are associated with sharply increasing zircon-melt partition coefficients of Th and U in a volatile oversaturated system (Claiborne et al., 2006; Bacon et al., 2007; Erdmann et al., 2013). In addition, the high Th and U contents is most likely the reason for the metamictization of the type-2 zircons, as self-irradiation by radioactive decay of Th and U results in crystal structure damage causing a low crystallinity and common Pb loss (Nasdala et al., 2001; Geisler et al., 2007; Zeng et al., 2017). (3) The type-2 zircons show significantly higher Hf contents and lower Zr/Hf mass ratios (10–30) than the type-1 magmatic zircons (Fig. 8). This indicates that Hf is incorporated into the microporous type-2 zircon as a result of fluid circulation, i.e. type 2 zircons were generated in a volatile-rich environment (e.g. Qu et al., 2019). (4) The non-CHARAC REE behavior in type-2 zircons is an indication of its formation in a magmatic-hydrothermal environment rather than in silicate melts (Bau, 1996; Zeng et al., 2017). (5) The porous texture and low crystallinity of the type-2 zircons are consistent with zircons formed by deuteric dissolution-precipitation in a magmatic-hydrothermal transition stage rather than by recrystallization (Yang et al., 2014). (6) The type-2 zircons generally show the same U-Pb ages as the type-1 zircons (Fig. 6)

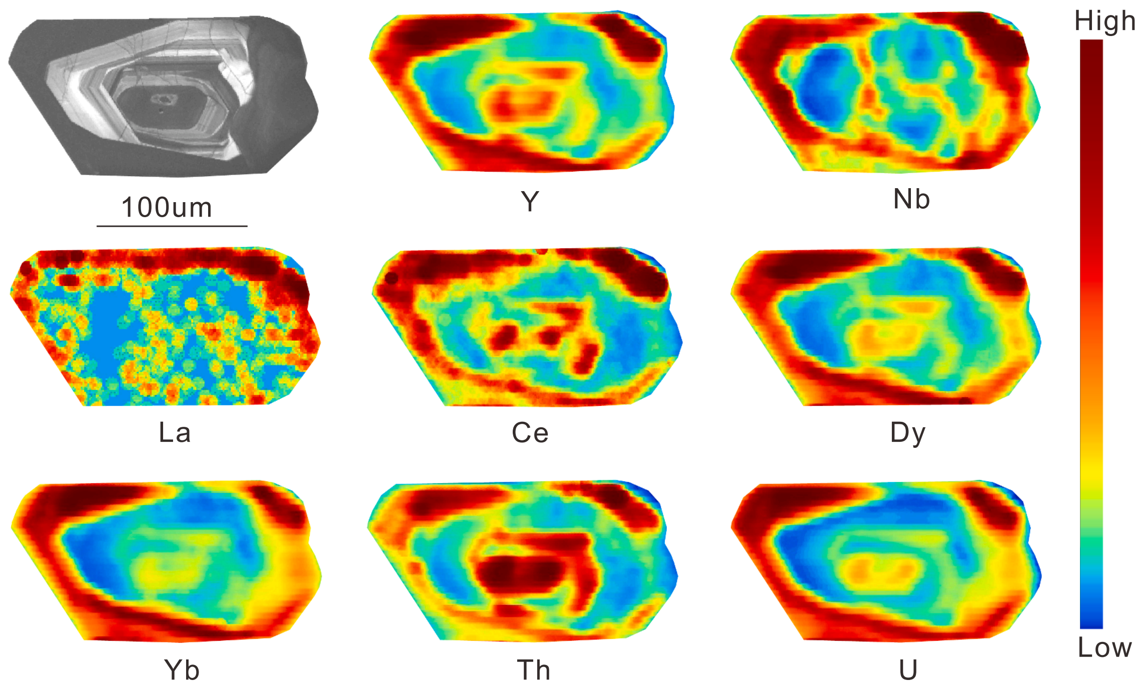

Fig. 10. Trace elemental mapping for a zircon from the Zudong granite. Zircons from Dabu and Xinfeng granites also show similar trace element geochemical compositions. Trace elements mapping for the zircon from the Dabu and Xinfeng granites are given in supplementary Figures.

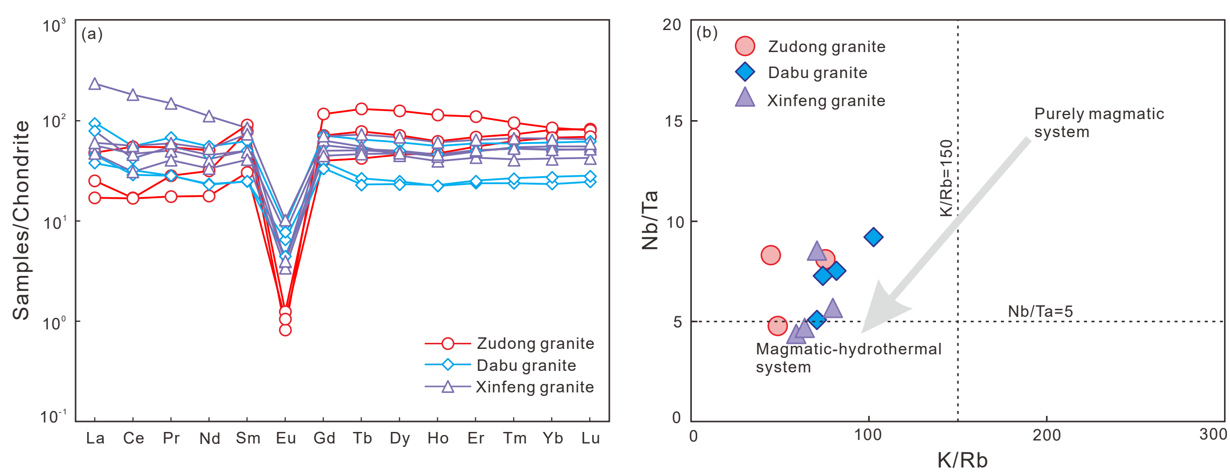

Fig. 11. (a) Normalized REE patterns and (b) Nb/Ta vs K/Rb diagrams for the whole-rock samples from the Zudong, Dabu, and Xinfeng granites.

indicating that the magmatic-hydrothermal stage during which the type-2 zircons were generated, was part of the magmatic event during which the type-1 zircons were formed.

The type-2 zircons are mostly characterized by total weight of the EMPA between 92 wt% and 97 wt%, which could be the evidence for the zircons generated in a volatile-rich condition (Breiter and Škoda 2012; Zeng et al., 2017), even though the high trace element contents might result that the total weight of the EMPA analyses for zircons were underestimated. The volatile content, increases during the magmatic-hydrothermal processes, which is also evidenced by the higher F contents in the type-2 zircons and the occurrence of muscovite, fluorite, topaz, and fluorocarbonate in the granites (Huang et al., 1989). Also, the F-rich hydrothermal fluid carried significant amounts of Zr, which explains the formation of type-2 zircon around type-1 zircon (e.g., Park et al., 2016; Zhao et al., 2018). All in all, the occurrence of the type-2 zircons indicates that the highly fractionated granite evolved to the volatile-oversaturated magmatic-hydrothermal stage. This conclusion is supported by the low Nb/Ta (4.37–9.21), Zr/Hf (13.1–27.6) and K/Rb (44.7–102.5) mass ratios of the granites (Fig. 11b; Breiter et al., 2014; Ballouard et al., 2016; Li et al., 2017; Wu et al., 2017b).

5.2. Factors controlling the generation of HREE ion-adsorption deposits

5.2.1. HREE enrichment relative to LREE

Fractional crystallization always proceeds during the magmatic evolution to a volatile-rich magmatic-hydrothermal stage and thus would have significant influence on the geochemical compositions of the minerals generated in the volatile-rich magmatic-hydrothermal stage. The relatively low Eu content in the type-2 zircons can be attributed to early plagioclase fractional crystallization, which removed Eu from the magmatic-hydrothermal system. Generally, HREEs have higher charge-to-ionic-radius ratios and are more incompatible than LREEs in rock-forming minerals in granites, which causes HREE enrichment relative to LREE in the magmatic-hydrothermal system after extensive fractional

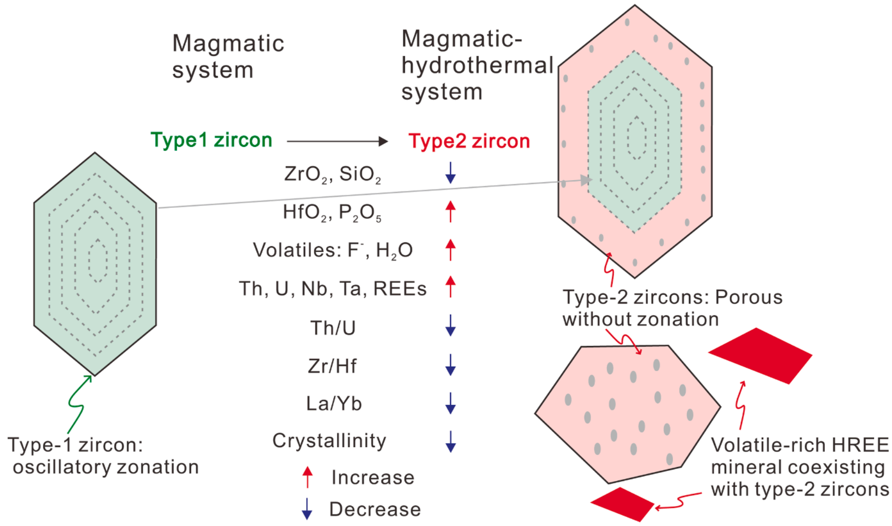

Fig. 12. Cartoon showing textural and geochemical characteristics of magmatic type-1 zircons (green) and hydrothermal type-2 zircons (pink).

crystallization (Gelman et al., 2014; Wu et al., 2017b). Therefore, although the type-2 zircons show higher contents of both LREE and HREE than the type-1 zircons, the relative increase of Y-Yb (HREE) from type-1 zircons to type-2 zircons is higher than the relative increase of La-Ce (LREE) as is evidenced by the elemental mapping (Fig. 10). It is also observed that the type-2 zircons show significantly higher Yb contents and display lower average La/Yb ratios than those of the type-1 zircons (Fig. 9d-f), manifesting the more enrichment of HREE relative to LREE in the magmatic-hydrothermal transition stage during which the type-2 zircons were generate. This inference is consistent with the geochemical composition of the granites hosting the HREE deposits as they show flat REE patterns and are characterized by low $(La/Yb)_N$ ratios (Fig. 11a).

HREE ion-adsorption deposits are characterized by relatively high HREE/LREE ratios in the weathering profile of the granites. However, weathering normally results in enrichment of LREEs relative to HREEs (Yusoff et al., 2013; Xu et al., 2017). Thus, a high HREE content relative to LREE in the parent granite in order to ensure a high HREE/LREE ratio in its weathering profile, is vital for the generation of the HREE ion-adsorption deposit. Indeed, as well as the Zudong, Xinfeng and Dabu granites, all parent granites for the HREEs ion-adsorption deposit in South China show flat HREE patterns and high HREEs/LREEs ratios (Li et al., 2017). Therefore, enrichment of HREE relative to LREE in the magmatic-hydrothermal stage should be critical for the formation of HREE dominated ion-adsorption deposits.

5.2.2. *Volatile-rich conditions*

The occurrence of type-2 zircons implies volatile oversaturation in the magmatic-hydrothermal system, which could be another critical factor that promotes HREE mineralization during weathering. Generally, zircon, xenotime, fergusonite, and titanite are the main HREE-hosted minerals in the volatile-undersaturated magmatic processes for granites. However, zircon, xenotime, and fergusonite are insoluble during weathering processes and can, therefore, not effectively release $HREE^{3+}$ (Huang et al., 1989; Bao and Zhao, 2008; Li et al., 2017). Titanite could be the potential minerals released HREEs during weathering to generate ion-adsorption deposits (Sanematsu and Watanabe, 2016), but titanite is absent in the Zudong, Dabu, and Xinfeng granites. Further, titanite is usually accompanied by the occurrence of allanite in the granites in South China and the weathering products of these granites are mostly dominated by LREEs rather than HREEs, e.g. the Bachi, Xiache, Laishi, and Shatian LREE-dominated ion-adsorption deposits (Chen and Yu, 1994; Hsieh et al., 2008; Li et al., 2017; Zhao et al., 2021). In contrast, in a volatile-oversaturated magmatic-hydrothermal system, the HREEs could be hosted in the volatile-rich REE minerals, such as synchysite-(Y), aeschynite-(Y), calcybeborosilite-(Y), and atelisite-(Y), which have been observed in the granites that are associated with these HREE-deposits (Fig. 3; Bao and Zhao, 2008; Sanematsu and Watanabe, 2016; Li et al., 2017). These volatile-rich REE minerals are easily dissolved during weathering and could be the main HREE source for the generation of the HREE-dominated ion-adsorption deposits.

5.2.3. *Extensional geodynamic setting in South China*

Our results show that the magmatic-hydrothermal stage of the granites is essential for the formation of HREE-dominated ion-adsorption deposits in South China. It is also noteworthy that the granites associated with HREE-dominated ion-adsorption in South China were generated in Late Jurassic-Cretaceous (e.g., Dabu, Xinfeng, Zudong, Datian, Xiawenting and Zhaibeiding HREE deposits; Liang et al., 2012; Shao et al., 2014; Li et al., 2017), during which South China underwent extension due to the slab foundering of the flat-subducted Paleo-Pacific plate beneath South China and high-angle subduction induced by slab roll-back (Li and Li, 2007; Li and Li, 2007), or in the Silurian (e.g., Shangyou HREE deposits), during which South China also underwent post-orogenic extension (Faure et al., 2009; Zhang et al., 2012). Generally, an extensional tectonic setting is favorable for the generation of highly fractionated granites progressing towards the magmatic-hydrothermal stage. Large-scale extensional structures provide a low-angle magma conduit allowing long-term magmatic migration and magmatic evolution (Wu et al., 2017b). In addition, the elevated geothermal gradient, which is induced by upwelling of the asthenosphere mantle in an extensional setting (Chen et al., 2016), also contributes to the generation of highly fractionated granites (Wu et al., 2017b). We, therefore, propose that the extensive extensional setting in South China contributes to the HREE mineralization potential of the granites.

In conclusion, the generation of the HREE-dominated ion-adsorption deposits in South China are associated with the following: (1) highly fractionated granites evolving to the magmatic-hydrothermal stage resulting in HREE enrichment relative to LREE; (2) the generation of volatile-rich HREE mineral phases in a volatile-rich environment, and (3) an extensional geodynamic setting promoting the generation of highly fractionated granites. In addition, the epigenetic process associated with a tropical climate and acidic soil water, which promotes the dissolution of the HREE-rich minerals and migration of the $HREE^{3+}$ to be adsorbed by clay minerals and Fe-Mn oxides, is also important.

Furthermore, the similar texture, crystallinity, and geochemistry of the zircons in the Zudon, Dabu, and Xinfeng granites that host the HREE ion-adsorption deposits (Fig. 12) imply that zircon can be a suitable path-finder mineral in evaluating the HREE ion-adsorption mineralization potential of granites.

6. Conclusions

Zircons from the Zudon, Dabu, and Xinfeng granites that host HREE-dominated ion-adsorption deposits can be subdivided into two types. Type-1 zircons in the Zudon, Dabu, and Xinfeng granites show similar characteristics, including oscillatory zonation, a high crystallinity, and relatively high Th/U and Zr/Hf ratios (Fig. 12). Type-2 zircons in the Zudon, Dabu, and Xinfeng granites also show similar characteristics, i.e. they are sometimes porous, do not show zonation, and have a low crystallinity (Fig. 12). The type-1 zircons are generated from a fractionated magma and the type-2 zircons are generated in a volatile-REE-rich magmatic-hydrothermal system, during which volatile-rich HREE minerals were also formed. The volatile-HREE-rich minerals dissolve during weathering generating HREE ion-adsorption deposits. The progression of the highly fractionated granites to the magmatic-hydrothermal stage is, therefore, vital for the generation of HREE ion-adsorption deposits. Consequently, zircon characterization can be an effective method to determine whether a granite has the potential to generate HREE ion-adsorption deposits.

Declaration of Competing Interest

The authors declare that they have no known competing financial interests or personal relationships that could have appeared to influence the work reported in this paper.

Acknowledgements

We thank editor-in-chief Huayong Chen and associate editor Taofa Zhou for handling our paper, and are grateful to three anonymous reviewers for their valuable comments that significantly improve our paper. This research was jointly funded by the Guangdong Major Project of Basic and Applied Basic Research (grant no. 2019B030302013), the Technology Planning of Guangdong Province, China (grant no. 2020B1212060055), and the Natural Science Foundation of Guangdong Province (No. 2022A1515010406). We would like to thank Dan Wu, Yonghua Cao, and Jingzhao Dou from the Guangzhou Institute of Geochemistry for their help with the analyses.

Appendix A. Supplementary data

Supplementary data to this article can be found online at https://doi.org/10.1016/j.oregeorev.2022.104931.

References

Bacon, C.R., Sisson, T.W., Mazdab, F.K., 2007. Young cumulate complex beneath Veniaminof caldera, Aleutian arc, dated by zircon in erupted plutonic blocks. Geology 35, 491–494.

Ballouard, C., Poujol, M., Boulvais, P., Branquet, Y., Tartèse, R., Vigneresse, J.-L., 2016. Nb-Ta fractionation in peraluminous granites: a marker of the magmatic-hydrothermal transition. Geology 44 (3), 231–234.

Bao, Z., Zhao, Z., 2008. Geochemistry of mineralization with exchangeable REY in the weathering crusts of granitic rocks in South China. Ore Geol. Rev. 33, 519–535.

Bau, M., 1996. Controls on the fractionation of isovalent trace elements in magmatic and aqueous systems: evidence from Y/Ho, Zr/Hf, and lanthanide tetrad effect. Contrib. Mineral. Petrol. 123, 323–333.

Breiter, K., Lamarão, C.N., Borges, R.M.K., Dall'Agnol, R., 2014. Chemical characteristics of zircon from A-type granites and comparison to zircon of S-type granites. Lithos. 192–195, 208–225.

Breiter, K., Škoda, R., 2012. Vertical zonality of fractionated granite plutons reflected in zircon chemistry: The Cínovec A-type versus the Beauvoir S-type suite. Geol. Carpath. 63, 383–398.

Černý, P., Teertstra, D.K., Chapman, R., Selway, J.B., Hawthorne, F.C., Ferreira, K., Chackowsky, L.E., Wang, X.J., Meintzer, R.E., 2012. Extreme fractionation and deformation of the leucogranite-pegmatite suite at Red Cross Lake, Manitoba, Canada. IV. Mineralogy. Can. Mineral. 50, 1839–1875.

Chakhmouradian, A.R., Wall, F., 2012. Rare earth elements: minerals, mines, magnets (and more). Elements 8, 333–340.

Charvet, J., Shu, L., Faure, M., Choulet, F., Wang, B., Lu, H., Le Breton, N., 2010. Structural development of the Lower Paleozoic belt of South China: genesis of an intracontinental orogen. J. Asian Earth Sci. 39, 309–330.

Chen, B., Yu, S., 1994. The geological and geochemical characteristics of late Yanshanian granites in Renju-Huangshe area, Pingyuan, Guangdong. Acta Sci. Nat. Univ. Sunyatseni. 33, 130–133 in Chinese with English abstract.

Chen, Y.X., Li, H., Sun, W.D., Ireland, T., Tian, X.F., Hu, Y.B., Yang, W.B., Chen, C., Xu, D. R., 2016. Generation of late mesozoic Qianlishan A2-type granite in nanling range, south china: implications for Shizhuyuan W-Sn mineralization and tectonic evolution. Lithos 266–267, 435–452.

Claiborne, L.L., Miller, C.F., Walker, B.A., Wooden, J.L., Mazdab, F.K., Bea, F., 2006. Tracking magmatic processes through Zr/Hf ratios in rocks and Hf and Ti zoning in zircons: an example from the Spirit Mountain batholith. Nevada. Mineral Mag. 70, 517–543.

Dou, J., Huang, X., Chen, F., 2021. Successive magma mixing in deep-seated magma chambers recorded in zircon from mafic microgranular enclaves in the Triassic Mishuling granitic pluton, Western Qinling, Central China. J. Asian Earth Sci. 207, 104656.

Erdmann, S., Wodicka, N., Jackson, S.E., Corrigan, D., 2013. Zircon textures and composition: refractory recorders of magmatic volatile evolution? Contrib. Mineral. Petrol. 165, 45–71.

Fan, H.R., Niu, H.C., Li, X.C., Yang, K.F., Yang, Z.F., Wang, Q.W., 2020. A preliminary review on the types, ore genesis and resource perspective of endogenic REE deposits in China. Chin. Sci. Bull. 65, 1–16.

Fan, W., Wang, Y., Zhang, A., Zhang, F., Zhang, Y., 2010. Permian arc–back-arc basin development along the Ailaoshan tectonic zone: geochemical, isotopic and geochronological evidence from the Mojiang volcanic rocks, Southwest China. Lithos 119, 553–568.

Faure, M., Shu, L., Wang, B., Charvet, J., Choulet, F., Monie, P., 2009. Intracontinental subduction: a possible mechanism for the Early Palaeozoic Orogen of SE China. Terra Nova 21, 360–368.

Fu, W., Li, X.T., Feng, Y.Y., Feng, M., Peng, Z., Yu, H.X., Lin, H., 2019. Chemical weathering of S-type granite and formation of Rare Earth Element (REE)-rich regolith in South China: critical control of lithology. Chem. Geol. 520, 33–51.

Geisler, T., Schaltegger, U., Tomaschek, F., 2007. Re-equilibration of zircon in aqueous fluids and melts. Elements 3, 43–50.

Gelman, S.E., Deering, C.D., Bachmann, O., Huber, C., Gutiérrez, F.J., 2014. Identifying the crystal graveyards remaining after large silicic eruptions. Earth Planet. Sci. Lett. 403, 299–306.

Hoskin, P.W., 2005. Trace-element composition of hydrothermal zircon and the alteration of Hadean zircon from the Jack Hills, Australia. Geochim. Cosmochim. Acta 69, 637–648.

Hoskin, P.W., Schaltegger, U., 2003. The composition of zircon and igneous and metamorphic petrogenesis. Rev. Mineral. Geochem. 53, 27–62.

Hsieh, P.S., Chen, C.H., Yang, H.J., Lee, C.Y., 2008. Petrogenesis of the Nanling Mountains granites from South China: constraints from systematic apatite geochemistry and whole-rock geochemical and Sr-Nd isotope compositions. J. Asian Earth Sci. 33, 428–451.

Huang, D., Wu, C., Han, J., 1989. REE geochemistry and mineralization characteristics of the Zudong and Guanxi granites, Jiangxi Province. Acta Geol. Sin. (English edition) 2, 139–157.

Huo, M., 1992. Distribution characteristics of the weathering-crust-type rare-earth resources in Nanling, China. J. Nat. Resources 7, 64–70 in Chinese with English abstract.

Kelly, C.J., Harlov, D.E., Schneider, D.A., Jackson, S.E., Dubosq, R., 2020. Experimental fluid-mediated alteration of zircon under lower greenschist facies conditions. Can Mineral. 58, 247–265.

Li, M.Y.H., Zhao, W.W., Zhou, M., 2017. Nature of parent rocks, mineralization styles and ore genesis of regolith-hosted REE deposits in south china: an integrated genetic model. J. Asian Earth Sci. 148, 65–95.

Li, M.Y.H., Zhou, M.F., Williams-Jones, A.E., 2019. The genesis of regolith-hosted heavy rare earth element deposits: Insights from the world-class Zudong deposit in Jiangxi Province, South China. Econ. Geol. 114, 541–568.

Li, X.H., Li, W.X., Li, Z.X., Liu, Y., 2008. 850–790 Ma bimodal volcanic and intrusive rocks in northern Zhejiang, South China: a major episode of continental rift magmatism during the breakup of Rodinia. Lithos 102 (1–2), 341–357.

Li, Z.X., Li, X.H., 2007. Formation of the 1300-km-wide intracontinental orogen and postorogenic magmatic province in Mesozoic South China: a flat–slab subduction model. Geology 35 (2), 179–182.

Liang, J., Qi, F., Fan, H., Ding, Y., 2012. The geochemical characteristics of Dabu rock mass and the relationship with tungsten mineralization. China Tungsten Ind. 27, 7–10 in Chinese with English abstract.

Mao, J., Cheng, Y., Chen, M., Franco, P., 2013. Major types and time-space distribution of Mesozoic ore deposits in South China and their geodynamic settings. Mine. Depos. 48, 267–294.

Middelburg, J.J., van der Weijden, C.H., Woittiez, J.R., 1988. Chemical processes affecting the mobility of major, minor and trace elements during weathering of granitic rocks. Chem Geol. 68, 253–273.

Nasdala, L., Wenzel, M., Vavra, G., Irmer, G., Wenzel, T., Kober, B., 2001. Metamictisation of natural zircon: accumulation versus thermal annealing of radioactivity-induced damage. Contrib. Mineral. Petrol. 141, 125–144.
Park, C., Song, Y., Chung, D., Kang, I.M., Khulganakhuu, C., Yi, K., 2016. Recrystallization and hydrothermal growth of high U-Th zircon in the Weondong deposit, Korea: record of post-magmatic alteration. Lithos. 260, 268–285.
Pettke, T., Audétat, A., Schaltegger, U., Heinrich, C.A., 2005. Magmatic-to-hydrothermal crystallization in the W-Sn mineralized Mole Granite (NSW, Australia): Part II: Evolving zircon and thorite trace element chemistry. Chem. Geol. 220, 191–213.
Qu, P., Li, N.B., Niu, H.C., Yang, W.B., Shan, Q., Zhang, Z.Y., 2019. Zircon and apatite as tools to monitor the evolution of fractionated I-type granites from the central Great Xing'an Range, NE China. Lithos 348, 105207.
Rudnick, R.L., Gao, S., 2003. Composition of the continental crust. Treatise on Geochemistry, vol. 3. Elsevier, Amsterdam, Netherlands, pp. 1–64.
Sanematsu, K., Kon, Y., Imai, A., Watanabe, K., Watanabe, Y., 2013. Geochemical and mineralogical characteristics of ion-adsorption type REE mineralization in Phuket, Thailand. Mine. Depos. 48, 437–451.
Sanematsu, K., Watanabe, Y., 2016. Characteristics and genesis of ion adsorption-type rare earth element deposits. Rev. Econ. Geol. 18, 55–79.
Shao, F., Xu, J.J., Hua, J., Nie, B., Lu, C., 2014. Geochemical characteristics and prospecting potential for uranium and tungsten of Dabu intrusion, Southern Jiangxi Province, China. Geol. Mineral Resources South China 30, 252–259 in Chinese with English abstract.
Sun, S.S., McDonough, W.F., 1989. Chemical and isotopic systematics of oceanic basalts: implications for mantle composition and processes. Geol. Soc. Lon. Sp. Pl. 42, 313–345.
Tang, J., Johannesson, K.H., 2010. Rare earth elements adsorption onto Carrizo sand: influence of strong solution complexation. Chem. Geol. 279, 120–133.
Tao, J., Li, W., Wyman, D.A., Wang, A., Xu, Z., 2018. Petrogenesis of Triassic Granite from the Jintan Pluton in Central Jiangxi Province, South China: Implication for Uranium Enrichment. Lithos 320–321, 62–74.
Wang, J., Ruan, D., 1989. Evolution and RE concentration of Heling-type RE acidic volcanic rock series. J. Chinese Rare Earth Soc. 7, 68–72 in Chinese with English abstract.
Wang, L.L., 2015. Geochemistry and petrogenesis of Early Paleozoic-Mesozoic granites in Ganzhou, Jiangxi Province, South China Block. PhD thesis, China University of Geosciences, Beijing, China, (in Chinese with English abstract).
Wang, X., Griffin, W.L., Chen, J., 2010. Hf contents and Zr/Hf ratios in granitic zircons. Geochem. J. 44, 65–72.
Wu, K.X., Zhu, P., Sun, T., Chen, L.K., Ouyang, H., Xiong, F., 2017a. Study on the ore-controlling factors and the mineralization and enrichment features of Dabu HREE deposit, Southern Jiangxi Province. Chinese Rare Earths 38, 1–10 in Chinese with English abstract.
Wu, F.Y., Liu, X.C., Ji, W.Q., Wang, J.M., Yang, L., 2017b. Highly fractionated granites: recognition and research. Sci. China Ser. D. 60, 1201–1219.
Xu, C., Kynický, J., Smith, M.P., Kopriva, A., Brtnický, M., Urubek, T., Yang, Y.H., Zhao, Z., He, C., Song, W.L., 2017. Origin of heavy rare earth mineralization in South China. Nat. Commun. 8, 1–7.
Yan, L.L., He, Z.Y., Klemd, R., Beier, C., Xu, X.S., 2020. Tracking crystal-melt segregation and magma recharge using zircon trace element data. Chem. Geol. 542, 119596.
Yang, W.B., Niu, H.C., Shan, Q., Sun, W.D., Zhang, H., Li, N.B., Jiang, Y.H., Yu, X.Y., 2014. Geochemistry of magmatic and hydrothermal zircon from the highly evolved Baerzhe alkaline granite: implications for Zr-REE-Nb mineralization. Mine. Depos. 49, 451–470.
Yusoff, Z.M., Ngwenya, B.T., Parsons, I., 2013. Mobility and fractionation of REEs during deep weathering of geochemically contrasting granites in a tropical setting, Malaysia. Chem. Geol. 349, 71–86.
Zeng, L.J., Niu, H.C., Bao, Z.W., Yang, W.B., 2017. Chemical lattice expansion of natural zircon during the magmatic-hydrothermal evolution of A-type granite. Am. Miner. 102, 655–665.
Zhang, F., Wang, Y., Zhang, A., Fan, W., Zhang, Y., Zi, J., 2012. Geochronological and geochemical constraints on the petrogenesis of Middle Paleozoic (Kwangsian) massive granites in the eastern South China Block. Lithos 150, 188–208.
Zhang, L., Wu, K.X., Chen, L.K., Zhu, P., Ouyang, H., 2015. Metallogenic features of ion-adsorption type REE deposits in Southern Jiangxi Province. J. Chin Soc. Rare Earths 33, 10–17 in Chinese with English abstract.
Zhang, Z., Zheng, G., Takahashi, Y., Wu, C., Zheng, C., Yao, J., Xiao, C., 2016. Extreme enrichment of rare earth elements in hard clay rocks and its potential as a resource. Ore Geol. Rev. 72, 191–212.
Zhao, X., Li, N.B., Huizenga, J.M., Yan, S., Yang, Y.Y., Niu, H.C., 2021. Rare earth element enrichment in the ion-adsorption deposits associated granites at Mesozoic extensional tectonic setting in South China. Ore Geol. Rev., 104317
Zhao, Z.D., Liu, D., Wang, Q., Wang, Q., Zhu, D.C., Dong, G.C., Zhou, S., Mo, X.X., 2018. Zircon trace elements and their use in probing deep processes. Earth Sci. Front. 25, 124–135.
Zheng, Y.F., Chen, R.X., Zhao, Z.F., 2009. Chemical geodynamics of continental subduction-zone metamorphism: insights from studies of the Chinese Continental Scientific Drilling (CCSD) core samples. Tectonophysics 475, 327–358.
Zhou, X.M., Sun, T., Shen, W.Z., Shu, L.S., Niu, Y.L., 2006. Petrogenesis of Mesozoic granitoids and volcanic rocks in South China: a response to tectonic evolution. Episodes 29, 26.